Size Quantization in Electrodeposited CdTe Nanocrystalline Films

Yitzhak Mastai and Gary Hodes*

Department of Materials and Interfaces, The Weizmann Institute of Science, Rehovot 76100, Israel

Received: October 7, 1996; In Final Form: December 5, 1996[⊗]

We describe the deposition and characterization of nanocrystalline CdTe films which exhibit size quantization. The CdTe films were electrodeposited from a dimethylsulfoxide solution of tri-(*n*-butyl)phosphine telluride and cadmium perchlorate at 100 °C. The stoichiometry of the films depends on applied potential and solution composition. The films contained about 5−10% Te excess and exhibited small blue shifts (0.1−0.2 eV) in their optical spectra. XRD and electron microscopy indicated a typical crystal size of ca. 8 nm. Pulse reverse plating was used to improve the film stoichiometry. The nanocrystal size could be controlled by the pulse parameters, and almost stoichiometric films with average crystal sizes from 4 to 7 nm were obtained, showing increases in bandgap up to 0.8 eV. Annealing the films resulted in gradual crystal growth and corresponding spectral red shifts until the bulk bandgap was reached. X-ray photoelectron spectroscopy (XPS) showed phosphorous incorporation in the films. The small crystal size was attributed to capping of the depositing CdTe by phosphine groups and could be controlled by the duty cycle of the plating pulsed current, whereby a longer off-time allowed more efficient capping and therefore smaller nanocrystal size.

Introduction

Size quantization in semiconductor colloids dispersed in a liquid or solid phase is an active field, due largely to the size-dependent electronic structure of these semiconductors.[1] Although far less extensively studied, size quantization in films of nanocrystalline semiconductors is becoming an increasingly active subsection of this field (ref 2 includes a review of size-quantized semiconductor films). Size quantization in these systems has been demonstrated for many different semiconductors, but a large part of the published work has concentrated on CdSe and CdS. Only a few examples of size quantization of CdTe have been described in the literature[3−7] and, to the best of our knowledge, only two of these deal with films: one, an ultrathin film deposited by injection of H_2Te into an aqueous solution of Cd^{2+} ions,[3] and the second, CdTe deposited in a Langmuir−Blodgett film.[4] Reference 7 describes films deposited by spraying a CdTe nanocrystalline dispersion onto heated substrates; while the precursor dispersion exhibited pronounced size quantization, the grain size in the films increased, because of the heating step, to ≥9 nm, at which size only small quantum effects are expected, although such effects were not explicitly discussed in this work. Another investigation on sputter-deposited CdTe films suggested size quantization as one of the possible reasons for the slightly increased bandgap of their samples.[8]

Chemical solution deposition (CD), one of the methods used to deposit nanocrystalline films, cannot be used to deposit CdTe (apart from the example given in ref 3 above, which can be considered to be a form of CD, if not in the usual sense) since no suitable tellurium source is known up to now. The organic electrodeposition technique used to deposit nanocrystalline CdSe and CdS[9] has not been successful in depositing similar films of CdTe. We have not succeeded in depositing CdTe from elemental Te in DMSO (we were unable to dissolve any appreciable amount of Te in DMSO), and in those cases where such deposition was reported,[10,11] the crystal size was, at least in some cases, reported to be large. Most other methods of electrodepositing CdTe using aqueous TeO_2 baths[12] or organic $TeCl_4$ baths[13−15] resulted, in our hands, in crystallite sizes of at least 20 nm, where no size quantization would be expected (the Bohr diameter of CdTe, which indicates the size above which no size quantization is expected, is ca. 15 nm).

One electrodeposition technique which did suggest smaller crystal sizes was described where tri-*n*-butylphosphine (TBP) was used to complex elemental Te in propylene carbonate.[16,17] The as-deposited films were reported to be X-ray amorphous, and even after annealing at 400 °C, the crystal size was only 50 nm.

We report here on nanocrystalline films of CdTe obtained using a simplified version of this technique. Furthermore, by using reverse pulse plating, better stoichiometry and a smaller crystallite size has been obtained. Band gaps up to 2.3 eV, an increase of 0.8 eV over the bulk band gap of CdTe, have been obtained for these quantized CdTe films.

Experimental Section

Deposition. *Substrates.* Substrates were titanium (Alfa) or indium-tin oxide coated glass (ITO), (Balzers, resistance ca. 10 Ω/sq). They were cut into 10 × 40 mm pieces, cleaned with aqua regia and sonicated in acetone. Prior to electrodeposition, the substrates were cleaned with distilled water and dried under a stream of argon.

Film Deposition. The deposition process was modified from the one originally used by Cocivera *et al.*[16,17] Tri-*n*-butylphosphine telluride (BPT) was prepared *in situ* in the deposition bath by making up a solution 60 mM tri-*n*-butylphosphine (BP) and 20 mM of elemental tellurium powder in 30 mL of dimethyl sulfoxide (DMSO) dried over molecular sieve. The solution was heated to 110 °C under a nitrogen atmosphere with vigorous stirring. After 2 h, the solution acquired a yellow color. The temperature was lowered to 100 °C, 4 mM of $Cd(ClO_4)_2$ was added, and 0.1 M $LiClO_4$ was used as a supporting electrolyte. All solids used in the deposition were vacuum dried at 100 °C for at least 12 h prior to use. Thin films of CdTe were deposited in a cell in which the anode and cathode were separated by a glass frit. A Pt anode was used and a saturated calomel electrode (SCE) served as the reference electrode. During electrodeposition, the solution was kept under a nitrogen

[⊗] Abstract published in *Advance ACS Abstracts,* March 1, 1997.

S1089-5647(96)03069-6 CCC: $14.00

atmosphere. All the experiments described here were carried out at 100 °C. Deposition was carried out under constant potential in the range of −650 to −1600 mV (vs SCE). Electrodeposits at various Cd/BPT concentrations were tested before choosing the preferred Cd/BPT ratio. Electrodeposition in several other solvents (see Results section) was tried before DMSO was chosen as the best solvent. Pulse electrodeposition was performed in a solution contained 4 mM $Cd(ClO_4)_2$, 20 mM tellurium, 60 mM BP, and 0.1 M $LiCiO_4$. A function generator (Tabor Electronics Ltd., Model 8122) was coupled to a potentiostat (Wenking MP75).

Characterization Methods. *Cyclic Voltammetry*. Cyclic voltammograms were obtained from a conventional three electrode cell, connected to a potentiostat (Wenking MP75) and an electrochemical programmer (Wenking VSG83) and a Houston Instruments 100 recorder.

Optical Spectra. The optical transmittance and reflectance spectra of the CdTe films were recorded using a Cary 17D infrared−visible or Uvikon 810 spectrophotometer. All optical spectra were recorded at room temperature in the 350−900 nm range. The spectra are shown in transmission mode corrected for specular reflection using the approximation T(corrected) = T(measured)/(1 − R).

X-ray Diffraction. Powder X-ray diffraction (XRD) spectra of films deposited on ITO glass and Ti were obtained using a Rigaku RU-200 B Rotaflex diffractometer operating in the Bragg configuration using Cu Kα radiation. Data were collected for 2θ from 15° to 55° with a counting rate of 0.25° min^{-1} and sampling interval of 0.002°. The accelerating voltage was set at 50 kV with a 160 mA flux. Scatter and diffraction slits of 0.3 and 0.5 mm collection slits were used.

Transmission Electron Microscopy (TEM). A Philips EM-400T electron microscope operating at 100 kV was used for TEM and electron diffraction (ED) in the selected area mode. Samples for TEM analysis were prepared by floating the films in aqueous HF (5%). The floated films were lifted onto copper G-300 (mesh) grids. Electron diffraction patterns were generated at a camera length of 800 nm.

X-ray Photoelectron Spectra (XPS). The XPS surface analysis was carried out using a AXIS HS Kratos XPS/Auger surface analysis system. All spectra were obtained with Mg Kα radiation. The vacuum in the analyzer chamber was of the order of 10^{-9} Torr. Charge correction was calibrated from the observed carbon 1s binding energy.

Results and Discussion

1. Influence of the Experimental Conditions. *Effect of the Deposition Solvent*. The original solvent used in the work of Cocivera *et al.*[16,17] was propylene carbonate, but since this solvent starts to polymerize at 110 °C, we could not perform the organic reaction between Te and BP in situ, since this reaction required at least 3 h at 110 °C. For this reason, we explored the use of other solvents. In acetonitrile and *N*,*N*-dimethylacetamide, the yield of the BPT complex was very low and films deposited in these solutions were heavily contaminated with Cd. Films deposited from ethylene glycol and diethylene glycol were often nonuniform, not smooth, and could not be grown to thicknesses greater than 200 nm. In addition, the BPT complex was unstable in those solvents and after a few films were deposited, yellow crystals, identified by infrared spectroscopy and XRD as a BPT complex, precipitated out from the solution. All the above problems were avoided by using DMSO. Films prepared in DMSO were uniform and smooth, the BPT complex was very stable, and electrodeposition could be carried out at temperatures of 110 °C and below. It should be noted that cyclic voltammetry obtained in all solvents showed similar electrochemical behavior with small shifts typical of solvent effects.

Solution Composition. The BPT/Cd ratio in the electrodeposition bath was important; variation in the film composition (Te/Cd) could be obtained by control of the BPT/Cd ratio. A series of experiments was made in which the BPT/Cd ratio was varied. We estimated the BPT concentration from the amount of BP and Te in the solution assuming a yield of 100%, although others reported a yield of ca. 45%[18] and in all cases, some unreacted tellurium was present in the solution. Films deposited from solutions with a BPT/Cd ratio of 4 and below were found to be Cd-rich. For a BPT/Cd ratio between 5 and 10, films of reasonable, although not perfect, stoichiometry were obtained, while for higher ratios, Te-rich films resulted. The presence of BP in large excess tends to inhibit deposition.

Plating Parameters. *(a) Deposition Potential*. Cathodic deposition of CdTe was carried out potentiostatically from an electrodeposition bath containing 4 mM $Cd(ClO_4)_2$, 20 mM Te, 60 mM BP, and 0.1 M $LiClO_4$ as supporting electrolyte at 100 °C. The presence of any free Cd or Te in the films could be seen by XRD. At deposition potentials between −900 and −1000 mV, the deposited films were Cd-rich. The subbandgap optical transmission of the films was low (which could be expected due to the presence of free cadmium). At deposition potentials between −1400 and −1600 mV, the deposited films were always Te-rich (although they were commonly Te-rich even at −1100 mV). In the potential range of −1100 to −1400 mV, the composition of the films was independent of the applied potential and depended on the relative BPT/Cd concentrations as described above. It was difficult to obtain stoichiometric films reproducibly. The plating current decreased with time and the rate of current decrease in this potential range was also affected by the BPT/Cd ratio. For example at a BPT/Cd ratio of 6, the deposition current dropped from an initial value of 1.5 to 0.15 mA cm^{-2} after 10 min, whereas this decrease took only about 2 min for a BPT/Cd ratio of 2. Although the current decreases with time, it was possible to grow fairly thick films (ca. 300 nm) using an appropriate BPT/Cd ratio. Electrodeposition at lower temperatures (50 and 25 °C) was carried out. We did not find any appreciable difference in crystal size or film composition compared to films deposited at 100 °C, but the deposition current at those lower temperatures was very low. The efficiency of the electrodeposition, estimated from the mass and the surface area of the film and assuming a two electron reduction step, is about 90−95%.

(b) Pulse Deposition. In order to improve the stoichiometry of the films, we investigated the use of pulse reverse deposition, whereby CdTe was deposited during a cathodic pulse and excess Te or Cd would be removed by a more positive pulse. Cyclic voltammetry (CV) was used to find the potential regions where CdTe would be deposited and Te and Cd stripped. The main CdTe deposition wave occurred at a potential of ca. −1100 mV (on both the bare ITO substrate as well as a CdTe-covered one), although there was a very slow current increase starting well positive of this value. Using solutions containing only BP/Cd^{2+} or BPT as active species, the Cd-stripping current was found to peak at −600 mV while Te-stripping peaked at −1150 mV. Predeposited Te held at −1200 mV visibly disappeared from the electrode, although films deposited at this potential normally contained excess Te. CdTe dissolution did not begin to occur until potentials positive of −200 mV were reached. On the basis of these measurements, we chose the more negative pulse, E_c, to be −1100 mV and the more positive pulse, E_a, to be −550 mV. The duty cycle (cathodic pulse width:anodic pulse

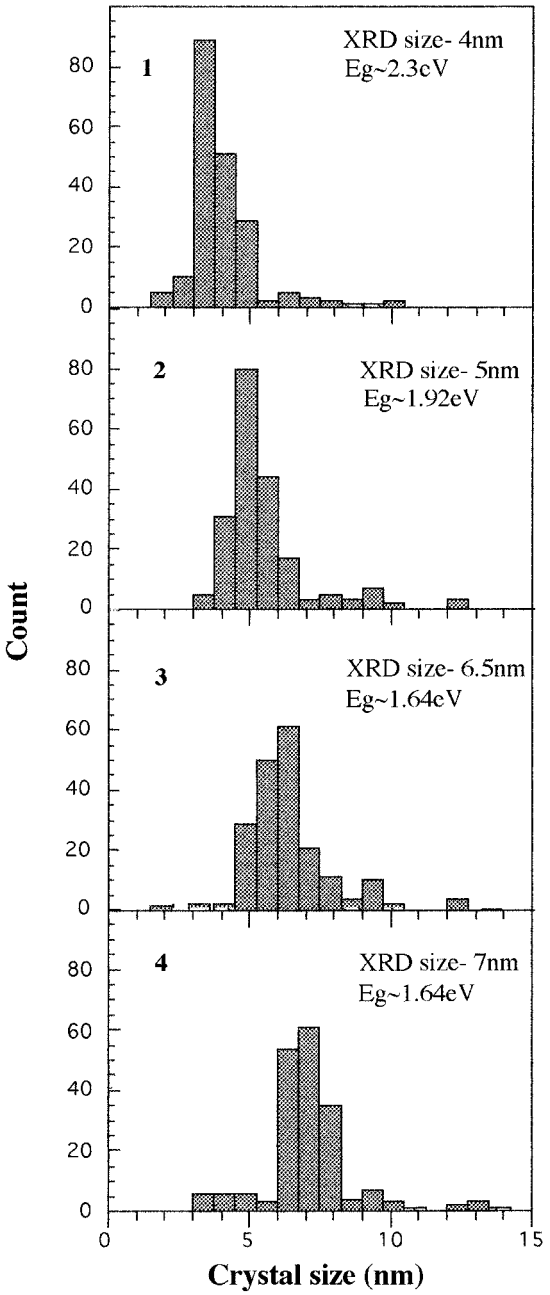

Figure 1. Crystal size distributions of four CdTe films, ca. 100 nm thick, deposited at 1 Hz with ratios of pulse on:pulse off (t_c/t_a) of (**1**) 0.25, (**2**) 0.38, (**3**) 0.5, and (**4**) 1.0. Crystal sizes measured by XRD peak broadening and bandgaps estimated from the optical spectra (Figure 2) are also shown.

width ratio) is defined here as t_c/t_a. The deposition was carried out with a pulse frequency of 1 Hz.

The films were indeed found to be more stoichiometric than those deposited under steady state conditions (little or no free Cd or Te was observed in the XRD patterns). In addition, the size distribution of the CdTe crystals was narrower than for dc plating, and the size of the nanocrystals could be controlled by the pulse parameters (see below).

2. Crystal Size and Optical Spectra—Size Quantization. Figure 1 shows the size distributions, measured from TEM micrographs, of four films deposited by pulse plating. The only difference in plating conditions between the films is the duty cycle of the pulse regime, given in the figure legend. Also given in the figures is the crystal size estimated from the XRD peak broadening and bandgap (estimated from optical spectra, see below). From these distributions, the average crystal sizes

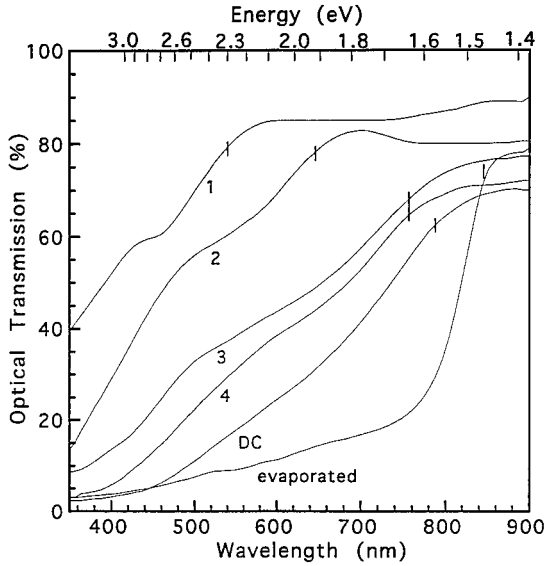

Figure 2. Optical transmission spectra (corrected for specular reflectance) of the four films from Figure 1, a constant potential (dc)-plated film (ca. 100 nm thick) and an evaporated CdTe film (ca. 200 nm thick; nonquantized as a comparison). Estimated values of E_g are shown. The loss in transmission at wavelengths longer than the bandgap energy (ca. 20%) can be ascribed mainly to diffuse scattering and possibly some absorption by small amounts of free Td or Cd.

for the four films are 4, 5, 6.5, and 7 mm. Three other films deposited under conditions employed for the 4 nm crystal size film in Figure 1 all had average crystal sizes, measured from TEM micrographs, in the range between 4.0 and 4.2 nm and with ≥80% of the crystals in the 3−5 nm range, demonstrating the good reproducibility of the method. Dc-plated films exhibit a very irreproducible morphology with widely-varying sizes and also various shapes. For this reason, it is difficult to give a quantitative size distribution of such films. Some crystals were as large as 20 nm while others were smaller than 5 nm. In addition, needles were commonly found in these films. Since no ED pattern could be found for these needles (they were not seen in dark-field imaging), and since Te was normally present in excess, it is likely that they were amorphous Te or, somewhat less likely, amorphous CdTe. XRD of these films gave an estimated crystal size of 8 nm and this value was reflected in the *typical* size seen by TEM.

Optical transmission spectra for the above four films, as well as a dc-plated film and a nonquantized evaporated CdTe film (typical crystal size 150−200 nm), are shown in Figure 2. The estimation of E_g ($1S_{3/2}-1S_e$ transitions) by extrapolating $(\alpha h\nu)^2$ vs $h\nu$ plots, which gives reasonably straight lines and E_g values for CD CdSe and ED CdS (but not ED CdSe) size-quantized films,[19] does not give any consistent and meaningful plots or E_g values for these films; the value of the exponent for an approximately straight line plot varies between 0.5 and 1.0 for these size-quantized CdTe films. Since this graphical method is based on a bulk density of states, there is no *a priori* reason why it should be valid, and its apparent applicability for CD CdSe and ED CdS is presumably fortuitous. The shape of the plots should depend, more than any other factor, on the size distribution of the nanocrystals. While the choice of E_g is necessarily somewhat arbitrary due to the size distribution, we take E_g to be near the high-energy side of the absorption onset (i.e., transmission drop) as marked by the vertical lines in Figure 2. The gradual nature of these onsets is presumably due to the larger crystals in the distribution (as long as they are present in appreciable concentrations), while the steep part of the spectrum may be attributed to the dominant size. The estimated values

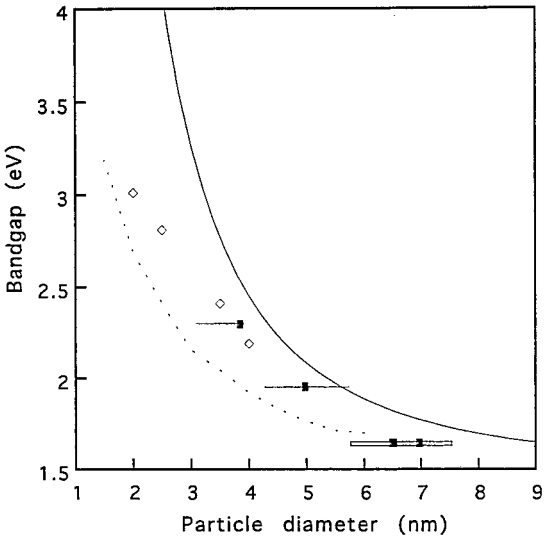

Figure 3. Bandgap of CdTe as a function of crystal size: (open diamonds) experimental results from ref 5; (horizontal bars) our experimental results measured from the TEM size distributions (the bar lengths represent the uncertainty due to size distribution; see text for explanation); the broad, open bar at 6−7 nm represents the larger uncertainty in determining E_g for films 3 and 4 from Figure 1; (filled squares) our results measured by XRD; (solid-line curve) simple effective mass model including Coulomb correction; (broken-line curve) theoretical model from ref 21.

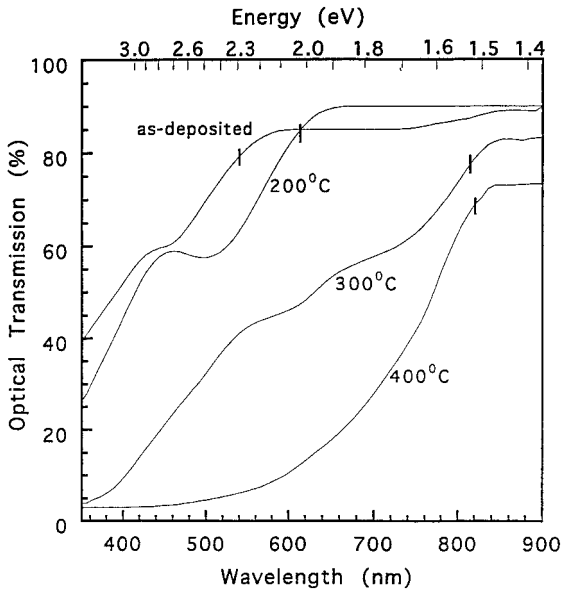

Figure 4. Optical transmission spectra (corrected for specular reflectance) of a pulse-plated CdTe film (film 1 in Figure 1) after annealing sequentially at various temperatures. The crystal sizes measured by XRD and estimated bandgaps are as-deposited: 4 nm and 2.3 eV; 200 °C: 5.5 nm and 2.02 eV; 300 °C: 16 nm and 1.52 eV; 400 °C: ca. 50 nm and 1.52 eV.

of E_g are the same for samples 3 and 4; this can be understood since the expected difference in E_g between a crystal size of 6.5 and 7.0 nm is small (ca. 0.05 eV, see Figure 3) and the estimation of E_g is approximate. We note that there is no obvious change in absorption coefficient (steepness of spectrum) with crystal size, in contrast to the situation observed in ref 5. For size-quantized, chemically-deposited CdSe films, we also find very little dependence of absorption coefficient on crystal size (see Figure 1 in ref 9), although the size-quantized films do have appreciably larger absorption coefficients than bulk (nonquantized) ones. We do not know whether this is due to the fact that our samples are aggregated or whether it is sample specific.

For films 1, 2, and 3, two clearly-separate onsets, separated by ca. 0.7 eV (films 1 and 2) and ca. 0.85 eV (film 3), are seen. The second, higher energy onset can be ascribed to the spin-orbit valence level to first conduction level transition ($1S_{1/2}-1S_e$). The spin−orbit splitting parameter in bulk CdTe (0.81 eV[20]) may be reduced to some extent on quantization due to the heavier split-off compared to light hole mass.

We can compare our results with theoretical models and other experimental results for the relationship between effective bandgap and CdTe nanocrystal size. The simple effective mass model for the change in effective bandgap (first optical transition) with crystal size is known to increasingly overestimate the bandgap as the crystal size becomes smaller. Lippens and Lannoo have used a tight-binding approximation to relate bandgap and size.[21] The results of their calculations, as well as that for the simple effective mass model, corrected for Coulomb effects, is shown in Figure 3 together with the experimental results of ref 5 for CdTe colloids and our present results. While the values of E_g can be estimated relatively accurately compared with the range of the bandgap values, the size distribution introduces a rather large uncertainty into the values of size. The horizontal bars represent the standard deviation calculated from the size distributions in Figure 1, but not including the small peaks. This manipulation is justified since a low concentration of larger crystals may affect the absorption onset somewhat, but the steep part of the absorption to a lesser degree, while the spectrum due to a low, or even medium concentration of smaller crystals will be swamped by that from the dominant, larger ones. Within the narrow region of overlap between our crystal sizes and those of ref 5, the two studies are in agreement (our results extend those of ref 5 to larger crystal sizes) and the experimental values fall in between the two theoretical models.

The above results show how the crystal size can be controlled by the deposition parameters. Annealing the films after deposition leads to crystal growth, and this allows another degree of control over size. Figure 4 gives optical transmission spectra of film 1 in Figure 1 as-deposited, and after annealing in nitrogen at various temperatures (the same sample was used for all the spectra, and annealed at successively higher temperatures), as a function of annealing temperature. The values of E_g estimated from these spectra and crystal sizes estimated from XRD spectra are also given in the figure legend for each annealing temperature. The 300 and 400 °C spectra give essentially bulk values of E_g. This is expected since the crystal size is equal to (300 °C) or larger than (400 °C) the Bohr diameter for CdTe, and therefore no strong size quantization effect on the bandgap is expected. We do not ascribe any relevance to the middle weak peak on the 300 °C spectrum other than to note that it could conceivably be due to smaller crystals in a bimodal distribution of crystal sizes; XRD would probably not show such a distribution. The 200 °C spectrum, with an E_g of 2.02 eV and crystal size (from XRD) of ca. 5.5 nm, is a little outside the experimental E_g vs size plot of Figure 3 and falls close to the effective mass model.

3. XPS Analyses of the Films—Phosphorous Incorporation. An XPS investigation of CdTe films deposited by both constant potential (dc plating) and pulse reverse electrodeposition was carried out. Two films were examined, one deposited at a dc potential of −1100 mV from a standard solution and the other using the pulse reverse method with the same parameters as film 1 in Figure 1. All the peaks from XPS spectra of those films were identified and attributed to Cd, Te, P, O, and C as well as small contributions (several %) from the

TABLE 1: XPS Peak Positions and Atomic Concentrations for dc-Plated and Pulse-Plated (t_c/t_a = 0.25) CdTe Films Deposited onto ITO Glass, before and after a 3 min Sputter Etch (ca. 30 nm Etched Away)[a]

		concentration (atom %)			
		dc plated		pulse plated	
elements	peak positions (eV)	as-deposited	sputter etch	as-deposited	sputter etch
C	284.20	57.56	33.33	59.91	50
O	531.16	29.24	42.62	26.09	27.67
	529.33				
	527.57				
	533.75				
Te	571.83	4.46	5.67	3.01	7.46
	573.71				
Te	575.41	0.88	0	1.47	0.6
Cd	404.40	5.79	5.14	4.62	9
P	131.50	1.41	0.78	1.55	1.79
Cd:Te:P atomic ratio		1:0.92:0.24	1:1.10:0.15	1:0.97:0.34	1:0.90:0.20

[a] The Cd:Te:P ratios are given for each film, before and after etching, normalized to unity Cd concentration. The total of the atomic concentrations, particularly for the etched films, is less than 100% due to the peaks from exposed substrate which are not included.

elements in the conducting glass substrates. The peak positions and atomic concentrations, both in the as-deposited film and after 3 mn Ar ion sputter etching (corresponding to ca. 30 nm depth), are listed in Table 1.

While many trends arise from the results shown in Table 1, we will concentrate on those which are most relevant for our present purposes. The Cd:Te ratios are close to unity (the accuracy of the technique does not justify reading any meaning into the differences; the Te concentrations are taken as the sum of the lower BE peaks [telluride] and higher BE peak [Te−O]). The most important conclusions are the relatively large amounts of P present in the films and the greater proportion of P present in the smaller crystal size films. This P can be ascribed to TBP adsorbed at the CdTe surface; the large C content is then due to the three butyl groups attached to the P, as well as to normal carbon contamination usually seen in these measurements. A 4.5 nm crystal (pulse-plated film) will have close to 20% of its atoms at the surface while the dc-plated film will have between 10 and 15% of its atoms at the surface. The concentrations of P are somewhat higher than this for the as-deposited films and comparable for the sputter-etched ones based on the assumption that one phosphorus is connected to each surface Te. This assumption is simplistic for several reasons. Steric considerations would suggest that there would be less surface-adsorbed P than expected. On the other hand, the possibility that binding may occur to both Cd and Te, as well as the possibility of more than a single adsorbed layer of phosphine, will give more P at the surface. The important point is not so much the absolute amounts of P in the films, but rather that the films do contain P in quantities approximately consistent with a surface-adsorbed species, and that the amount of P scales with the surface area of the nanocrystals. The P concentrations decreased with sputtering time, but even after 3 min of sputtering, both films still contained considerable amounts of P. The nanocrystalline films are presumably somewhat porous and the actual surface area is very different from the geometric one. It is therefore not surprising that a considerable amount of adsorbed species—this includes C and O as well as P—remains after sputtering.

It could be argued that O might be present in the bulk of the crystals and that the spectral blue shift is caused by some mixed Cd−Te−O compound. This is highly unlikely for two reasons. If it were true, annealing would not be expected to red shift the spectrum to that expected from bulk CdTe. Second, XRD peak positions of all samples are consistent with CdTe; they are not consistent with any known oxide of Cd and/or Te, all of which have (major) peak positions clearly separated from those of CdTe.

4. Mechanism of Nanocrystalline Growth and Size Control—Capping. We can consider three competing mechanisms of CdTe formation: Cd^0 deposition which reacts with BPT to give CdTe, reduction of BPT to Te^{2-} which reacts with Cd^{2+}, and direct discharge of a Cd−BPT complex, as proposed in ref 17. The first mechanism dominates at less-negative potentials (since the films in that potential region are Cd-rich) and the second at very negative potentials where excess Te is formed. For the third mechanism, stoichiometric films are expected.

The rather sharp decrease in plating current in the presence of phosphine is instructive. We find that a similar drop occurs for "CdSe" (see later) when deposited from a phosphine-containing bath, but not (or much less) for a similar bath without phosphine. This suggested inhibition of the deposition by excess phosphine by poisoning of the substrate surface (this includes the previously-deposited CdTe). The strong complexing ability of phosphines for chalcogenides would lead us to expect adsorption of the BP on Te sites of the growing CdTe film. In our case, the BP may act as a capping agent in much the same way as organic chalcogen compounds[22] and more specifically alkyl phosphines (and phosphine oxides)[23] used to limit colloidal growth. This means that during nucleation of CdTe on the electrode, BP reacts with the surface of CdTe and seals (caps) the surface, preventing further growth. In the case of colloids, it was suggested that phosphine oxides bind to cadmium atoms.[24] While we do not deliberately introduce any phosphine oxide, it is probable that appreciable amounts are present, either from small amounts of water or air present or by electrochemical oxidation of phosphine at the anode.

Pulse plating leads to an improvement of the film stoichiometry, and a reduction in the size distribution and control of the crystal size through the ratio between cathodic and anodic pulse durations. We showed that stoichiometric films were obtained using pulse reverse plating due to dissolution of elemental Cd or Te during the anodic pulse. However, another influence of the pulse plating compared to dc plating is the decrease in crystal size and improvement in the size distribution. On the basis of the mechanism of capping proposed above, we can understand the decrease in crystal size. The smallest crystal size was obtained at t_c/t_a ratio of 0.25. At this ratio, the electrode is held most of the time (80%) at a potential were deposition does not occur. Therefore during this relaxation time, the capping process can occur, while for dc deposition the capping process occurs together with the nucleation which reduces the efficiency of the former. Additionally, the capping can also prevent coalescence of two crystallites, thereby stabilizing small crystallites.

It could be argued that pulse plating itself is responsible for the decrease in crystal size. It is well-known that pulse plating of metals often results in grain refinement and this effect is usually explained by the very high rate of nucleation afforded by high plating currents for short (pulse on) times as well as high local adatom concentration.[25] New nucleation can occur at every pulse, not necessarily at the same nucleation sites, resulting in a decrease in the average crystal size, and adsorption of adatoms can block surface diffusion and growth. In our case, where the pulse-on times were relatively large (at least 200 ms), and current densities much lower (ca. 1 $mA \cdot cm^{-2}$) than usually used for pulse plating (at least 2 orders of magnitude higher is common), the first factor should not be so important. However, the high adatom (capping agent) concentration is relevant in our case. Thus, the different crystallite sizes shown in Figure 1 reflect the higher probability of capping the growing CdTe crystals with increasing off time (i.e., the more positive potential regime where no deposition occurs).

In an attempt to separate out the effects of pulse plating from capping, at least to some extent, we tried to carry out some analogous experiments with CdSe deposition. Unlike CdTe, CdSe could be deposited in the absence of BP, since Se dissolves to an appreciable extent (ca. 5 mM at 100 °C) in DMSO. (We were unable to deposit CdSe in the presence of BP under our experimental conditions; even 1 mM BP in the deposition solution resulted in a deposit which contained large amounts of Cd, even at very negative deposition potentials.) As for the CdTe, the perchlorate salt of Cd was used in order to minimize anion adsorption. Comparison was made between films, ca. 200 nm thick, deposited under dc conditions and 20% pulse-on conditions under the same temperature and approximately the same current density used for the CdTe films. The crystal size, measured by XRD, was found to be ca. 20 nm for the pulse-plated film compare to 30 nm for the dc-plated film. This effect could be explained by inefficient capping by other, less-adsorbing constituents of the plating solution. It is difficult to explain it by more rapid nucleation, since the same current density was used for the dc pulse plating (i.e., the *average* current during pulse plating was 20% of that during dc plating). In fact, some preliminary attempts by us to reduce crystal size by much higher current densities at much higher frequencies (which generally works successfully for metal deposition) met with only very limited success.

Conclusions

We show that nanocrystalline CdTe films can be grown by electrodeposition from DMSO solutions using tri-*n*-butylphosphine telluride as a Te source. Electrodeposition in the potential range of −1100 to −1400 mV gave films containing ca. 5−10% Te excess, with a typical crystal size of 8 nm but with a very large size and shape distribution. X-ray photoelectron spectroscopy measurements of the electrodeposited films showed phosphorus incorporation in the films. Using pulse-reverse plating resulted in stoichiomeric films with an average crystal size which could be controlled, by varying the pulse duty cycle, from 4 up to 7 nm, with the smaller size corresponding to a shorter deposition pulse time. All the films exhibited blue spectral shifts which correlated with the crystal size and could be explained by size quantization in the nanocrystals. A model of the deposition process and explanation of the influence of pulse plating on the film composition and crystal size has been proposed based on capping of the CdTe crystallites with strongly-adsorbed phosphine groups.

Acknowledgment. This work was supported under grant no. C13-219, Program in Science and Technology Cooperation, Human Capacity Development, Bureau for Global Programs, Field Support and Research, USAID, and by the Edith Reich Foundation.

References and Notes

(1) Yoffe, A. D. *Adv. Phys.* **1993**, *42*, 173.
(2) Gorer, S.; Hodes, G. In *Nanocrystalline Semiconductor Materials*; Kamat, P. V., Meisel, D., Eds.; Elsevier Press: New York, in press.
(3) Gallardo, S.; Gutierrez, M.; Henglein, A.; Janata, E. *Ber. Bunsenges. Phys. Chem.* **1989**, *93*, 1080.
(4) Grieser, F.; Neil Furlong, D.; Scoberg, D.; Ichinose, I.; Kimizuka, N.; Kunitake, T. *J. Chem. Soc., Faraday Trans.* **1992**, *88*, 2207.
(5) Rajh, T.; Micic, O. I.; Nozik, A. J. *J. Phys. Chem.* **1993**, *97*, 11999.
(6) Murray, C. B.; Norris, D. J.; Bawendi, M. G. *J. Am. Chem. Soc.* **1993**, *115*, 8706.
(7) Pehnt, M.; Schulz, D. L.; Curtis, C. J.; Jones, K. M.; Ginley, D. S. *Appl. Phys. Lett.* **1995**, *67*, 2176.
(8) Meléndez-Lira, M.; Jiménez-Sandoval, S.; Hernández-Calderón, I. *J. Vac. Sci. Technol. A* **1989**, *7*, 1428.
(9) Hodes, G. *Isr. J. Chem.* **1993**, *33*, 95.
(10) Rastogi, A. C.; Balakrishnan, K. S. *J. Electrochem. Soc.* **1989**, *136*, 1502.
(11) Balakrishnan, K. S.; Rastogi, A. C. *Sol. Energy Mater.* **1991**, *23*, 61.
(12) Panicker, M. P. R.; Knaster, M.; Kroger, F. A. *J. Electrochem. Soc.* **1978**, *125*, 566.
(13) Engelken, R. D.; Van Doren, T. P. *J. Electrochem. Soc.* **1985**, *132*, 2910.
(14) Gore, R. B.; Pandey, R. K. *Thin Solid Films* **1988**, *164*, 255.
(15) Pandey, R. K.; Razzini, G.; Bicelli, L. P. *Sol. Energy Mater. Sol. Cells* **1992**, *26*, 285.
(16) Darkowski, A.; Cocivera, M. *J. Electrochem. Soc.* **1985**, *132*, 2768.
(17) Von Windheim, J.; Cocivera, M. C. *J. Electrochem. Soc.* **1987**, *134*, 440.
(18) Zingaro, R. A.; Steeves, B. H.; Irglic, K. *J. Organomet. Chem.* **1965**, *4*, 320.
(19) Hodes, G.; Engelhard, T.; Albu-Yaron, A.; Pettford-Long, A. *Mater. Res. Soc. Symp. Proc.* **1990**, *164*, 81.
(20) Cardona, M. *J. Phys. Chem. Solids* **1963**, *24*, 1543.
(21) Lippens, P. E.; Lannoo, M. *Semicond. Sci. Technol.* **1991**, *6*, A157.
(22) Steigerwald, M. L.; Brus, L. E. *Annu. Rev. Mater. Sci.* **1989**, *19*, 471.
(23) Murray, C. B.; Norris, D. J.; Bawendi, M. G. *J. Am. Chem. Soc.* **1993**, *115*, 8706.
(24) Nirmal, M.; Murray, C. B.; Norris, D. J.; Bawendi, M. G. *Z. Phys. D* **1993**, *26*, 361.
(25) Choo, R. T. C.; Toguri, J. M.; El-Sherik, A. M.; Erb, U. *J. Appl. Electrochem.* **1995**, *25*, 384.